

Rotational Stiffness of Football Shoes Influences Talus Motion during External Rotation of the Foot

Feng Wei

Orthopaedic Biomechanics Laboratories,
Michigan State University,
East Lansing, MI, 48824,
e-mail: weifeng@msu.edu

Eric G. Meyer

Experimental Biomechanics Laboratory,
Lawrence Technological University,
Southfield, MI, 48076,
e-mail: emeyer@ltu.edu

Jerrod E. Braman

Orthopaedic Biomechanics Laboratories,
Michigan State University,
East Lansing, MI, 48824,
e-mail: bramanj1@msu.edu

John W. Powell

Department of Kinesiology,
Michigan State University,
East Lansing, MI, 48824,
powellj4@ath.msu.edu

Roger C. Haut¹

Orthopaedic Biomechanics Laboratories,
Michigan State University,
East Lansing, MI, 48824,
e-mail: haut@msu.edu

Shoe-surface interface characteristics have been implicated in the high incidence of ankle injuries suffered by athletes. Yet, the differences in rotational stiffness among shoes may also influence injury risk. It was hypothesized that shoes with different rotational stiffness will generate different patterns of ankle ligament strain. Four football shoe designs were tested and compared in terms of rotational stiffness. Twelve (six pairs) male cadaveric lower extremity limbs were externally rotated 30 deg using two selected football shoe designs, i.e., a flexible shoe and a rigid shoe. Motion capture was performed to track the movement of the talus with a reflective marker array screwed into the bone. A computational ankle model was utilized to input talus motions for the estimation of ankle ligament strains. At 30 deg of rotation, the rigid shoe generated higher ankle joint torque at 46.2 ± 9.3 Nm than the flexible shoe at 35.4 ± 5.7 Nm. While talus rotation was greater in the rigid shoe (15.9 ± 1.6 deg versus 12.1 ± 1.0 deg), the flexible shoe generated more talus eversion (5.6 ± 1.5 deg versus 1.2 ± 0.8 deg). While these talus motions resulted in the same level of anterior deltoid ligament strain (approximately 5%) between shoes, there was a significant increase of anterior tibiofibular ligament strain ($4.5 \pm 0.4\%$ versus $2.3 \pm 0.3\%$) for the flexible versus more rigid shoe design. The flexible shoe may provide less restraint to the subtalar and transverse tarsal joints, resulting in more eversion but less axial rotation of the talus during foot/shoe rotation. The increase of strain in the anterior tibiofibular ligament may have been largely due to the increased level of talus eversion documented for the flexible shoe. There may be a direct correlation of ankle joint torque with axial talus rotation, and an inverse relationship between torque and talus eversion. The study may provide some insight into relationships between shoe design and ankle ligament strain patterns. In future studies, these data may be useful in characterizing shoe design parameters and balancing potential ankle injury risks with player performance. [DOI: 10.1115/1.4005695]

Keywords: biomechanical study, ankle injury, talus eversion, ligament strain, computational model, motion analysis, ankle kinematics, footwear

Introduction

Acute injuries that occur to the ankle are among the most frequent musculoskeletal injuries in all levels of sports, and ligament sprains account for 75% of these injuries [1]. In young athletes, acute ankle trauma is responsible for 10% to 30% of all sports-related injuries [2]. Each year an estimated 1×10^6 persons present to physicians with acute ankle injuries [3]. Approximately 85% of ankle sprains involve the lateral ankle ligaments that are ascribed to excessive foot inversion [4,5]. In contrast, high ankle and medial ankle sprains occur less frequently, being diagnosed in 10% to 15% of cases [6,7]. As opposed to a lateral ankle sprain, high and medial ankle sprains are more problematic due to their potential for resulting in significantly greater time lost and subsequent chronic ankle dysfunction [7–11]. The mechanism of injury in high and medial ankle sprains is commonly ascribed to excessive internal rotation of the upper body, while the foot is planted on the playing surface [8].

Numerous studies have investigated the role of shoe design in the characteristics of shoe-surface interfaces [12–16]. While linear traction between a shoe's outsole and a sports surface is necessary

for high-level performance during any athletic contest, it is generally accepted that excessive rotational traction (torque) may result in ankle and knee injuries [15,17,18]. Additionally, Livesay et al. [19] also measured the rotational stiffness of shoe-surface combinations and showed that differences in rotational stiffness are often greater than differences in peak torque generated between various combinations. The study concludes that rotational stiffness of the shoe-surface interface may be another important risk factor for lower extremity injuries. A recent study by Villwock et al. [15], involving football shoes and various natural and synthetic playing surfaces, suggests that the shoe-surface rotational stiffness may be associated, in part, with the design of a shoe's upper. However, the effect of shoe design on the patterns of ankle ligament strain during external rotation of the foot has not been directly investigated to date.

Talus motion plays an important role in developing ankle ligament strains, especially under rotational loading [20], and therefore its motion is crucial in the study of potential mechanisms of ankle ligament sprain [21]. Recently, Wei et al. [22] developed a computational ankle model, based on a generic computer tomography (CT) scan of a cadaver foot, which was validated against experimental data from human cadaver ankles [23]. The model has been used to estimate ankle ligament strains and ankle joint torque during simulations of external foot rotation. In a more recent in vivo study by the same group [24], barefoot subjects performed single-legged, internal rotation of the body with a planted

¹Corresponding Author

Contributed by the Bioengineering Division of ASME for publication in the JOURNAL OF BIOMECHANICAL ENGINEERING. Manuscript received December 2, 2011; final manuscript received December 10, 2011; accepted manuscript posted January 25, 2012; published online April 2, 2012. Editor: Michael Sacks.

foot while a motion capture system tracked motion of the ankle. The kinematic data of the talus were then utilized to drive the computational model for estimation of the dynamic ankle ligament strains. The study showed the largest strains in the anterior tibiofibular (ATiFL) and anterior deltoid (ADL) ligaments, with strain peaking in the ATiFL prior to the ADL.

The purposes of the current study were (1) to evaluate a few football shoe designs in order to select two designs of significantly different rotational stiffness (i.e., the highest and the lowest), then (2) to conduct external rotation tests using human cadaver ankles in these two shoe designs in order to measure differences in talus motion for the same level of external shoe rotation, and finally (3) to input the talus kinematics into the validated computational model in order to estimate the differences in the patterns of key ankle ligament strains between these two extremes in shoe design. It was hypothesized that shoes with significantly different rotational stiffness would generate significantly different levels of torque and key ankle ligament strain patterns. These data would begin to show how differences in shoe design may influence differences in ankle ligament strains and potentially help guide studies on the role of shoe design in determining some of the mechanisms of ankle ligament injury during external rotation of the foot.

Methods

Shoe Stiffness Tests. Four football shoe designs were evaluated to determine their rotational stiffnesses (the rate at which torque is developed under rotation). Experiments were conducted on a custom, hydraulic, biaxial testing machine using a 244 Nm rotary actuator (Model SS-001-1V, Micromatic, Berne IN) and a vertically oriented linear actuator (Model 204.52, MTS Corp., Eden Prairie, MN). The four football shoe types were Nike Air, Nike Merciless, Adidas Blitz, and Nike Flyposite. A surrogate lower extremity was made of room temperature curing epoxy resin (Fiber Strand, Martin Senior Corp., Cleveland, OH) and a stainless steel rod (Fig. 1(a)). The surrogate foot was fitted in a left, size-10 shoe of each design. A football cleat mold (Fig. 1(b)) was made of the same epoxy material for each shoe and was inserted into an aluminum tray (Fig. 1(c)) which was secured to the rotation-locked linear actuator of the test machine with a custom fixture that allowed x-y adjustments to align the rod along with the linear and torsional actuators. The proximal end of the surrogate limb was inserted into an aluminum box (Fig. 1(c)) which was attached to the rotary actuator through a biaxial load cell (Model 1216CEW-2K, Interface, Scottsdale, AZ) with a capacity of 8896 N axial force and 113 Nm torsion (Fig. 1(c)). A pilot study, using a different load cell and shoes, showed that this

football cleat-mold structure can bear up to 200 Nm torque without observable damages to the shoe or the mold (data not shown).

A compressive pre-load of 1500 N and a rotational pretorque of 2 Nm were applied to the surrogate limb prior to internal rotation of the rod (external rotation of the foot). The magnitude of the preload was approximately two times body weight and selected to simulate weight bearing in a dynamic situation [23]. The pretorque was to ensure full contact between the medial edge of the foot and the shoe. A dynamic torque of 60 Nm was input in load control at a frequency of 1 Hz (0.5 s to peak torque) and repeated two more times for each shoe design. The loading portions of the torque-rotation curves were averaged across the three cycles and compared between shoes. The shoe rotational stiffness, defined as the slope of the torque-rotation curve (loading portion), was calculated in Nm/deg and also averaged and compared between shoes.

Cadaver Tests. Twelve (six pairs) fresh-frozen lower limbs from male cadavers (aged 56 ± 12 years) were used in these tests. The limbs were stored at -20°C and thawed to room temperature for 24 h prior to tests. The tibia and fibula were transected approximately 15 cm distal to the center of the knee. The proximal end of the tibia and fibula shafts were then cleaned with 70% alcohol and potted in an aluminum box with epoxy resin (Fig. 2(a)). Two screws were placed in the medial and lateral aspects of the proximal tibia, with an approximately 30 mm projected length, to help prevent the tibia from rotating within the potting material (Fig. 2(b)). From the shoe stiffness tests, shoes with the highest and lowest rotational stiffnesses were referred as the rigid and flexible shoes, respectively, and were randomly assigned to the left or right limbs. For each pair of feet, one foot was in the rigid shoe and the other was in the flexible shoe. Shoes were properly selected to fit the cadaver foot size and regular sports socks were used. The limb was then mounted upside down (foot pointing upward) in the test machine (Fig. 2(c)) with the same fixture as in the shoe stiffness tests.

The same preload (1500 N) and pre-torque (2 Nm) were applied along the axis of the tibia. Internal tibial rotations (external foot rotations) of 30 deg were input in position control at a frequency of 1 Hz (0.5 s to peak rotation). This rotation magnitude was selected based on a previous study [23] to ensure that no ankle failure/injury would occur during these tests. Only one trial for each cadaver foot was performed to eliminate any viscoelastic and micro-damage effects in the soft tissue. Maximum torques in the 30 deg of rotation tests were documented for each specimen. The loading portions of the torque-rotation curves and the slopes of their linear ranges (rotational stiffness in Nm/deg) were averaged across specimens and compared between shoes. Linear regression

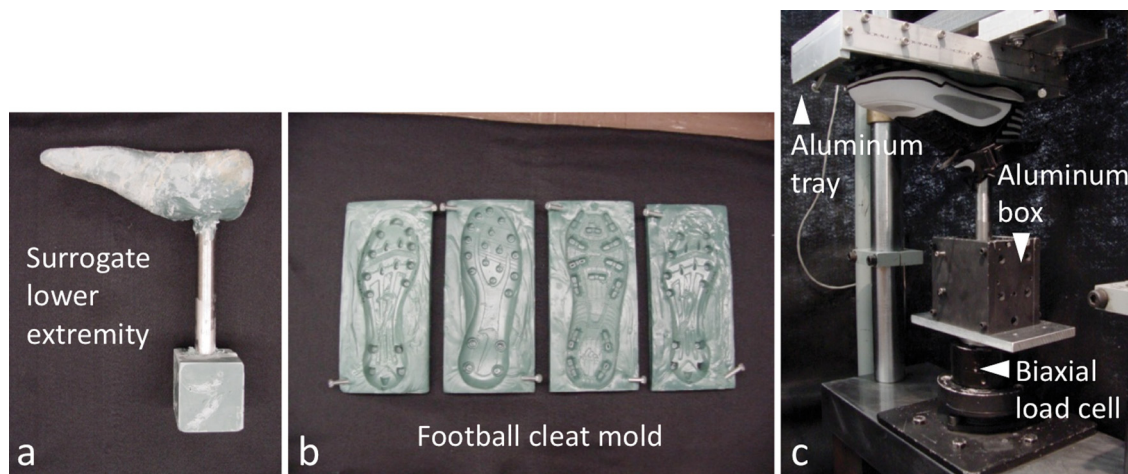


Fig. 1 Shoe stiffness tests preparation and setup. Surrogate lower extremity (a) and football cleat mold (b) were made of epoxy resin. A surrogate limb was attached to the testing machine through a biaxial load cell (c).

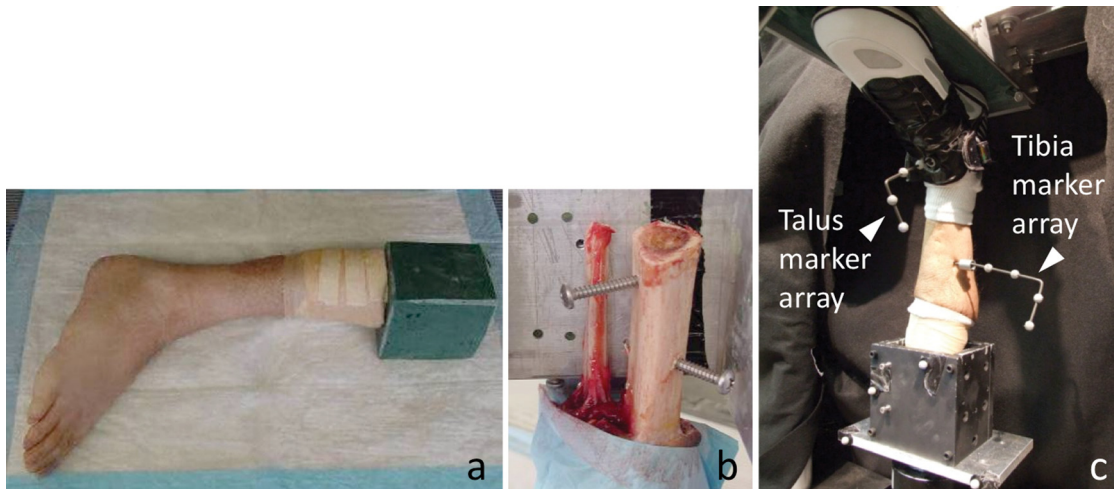


Fig. 2 Cadaver tests preparation and setup. The proximal end of the shank was potted using epoxy resin (a) with two screws placed earlier into the proximal tibia (b). A cadaveric limb with markers was mounted upside down into the testing machine (c).

was performed for the linear portion of each curve and the intercept along the rotation axis was documented and compared between shoes.

Motion Analysis. The cadaver tests were performed with two reflective marker arrays screwed into the talus and the tibia, respectively (Fig. 2(c)). These arrays were utilized in subsequent motion analyses of the talus with respect to the tibia using a five-camera Vicon motion capture system (Oxford Metrics Ltd., Oxford, United Kingdom) (Fig. 3). The talus array was attached from the anterior aspect of the ankle through a hole with a diameter of approximately 20 mm in the tongue of the shoe. Care was taken to avoid damage to the anterior deltoid ligament complex (a combination of the anterior tibiotalar and tibionavicular ligaments). The tibia array was positioned 10-20 cm proximal to its inferior articular surface (Fig. 2(c)). A joint coordinate system (JCS) was established based on each reflective marker array, as described in previous studies [22,25,26]. The translations and rotations of the talus relative to the tibia in three directions were determined in this JCS for the 30 deg of foot rotation test on each limb. Temporal profiles of talus rotation in different shoes were generated and compared with the actual shoe rotation.

Model Simulation. Talus motion data were used to drive a generic computational ankle model. Details of model development and motion simulation have been described in previous studies [22,24], thus only a brief description is given here. The ankle model was constructed from a generic CT scan of a cadaveric ankle with a separation of 0.6 mm between slices. CT images were first converted into 3D models in MIMICS (Materialise, Ann Arbor, MI) and then imported into dynamic rigid-body motion simulation software (SolidWorks, TriMech Solutions, LLC, Columbia, MD). This ankle model includes 21 ligaments formulated as linear elastic springs with properties adapted from the literature [22]. Ligament strains, defined in percentage as the relative elongations of ligaments, were estimated from the computational model.

Statistical Analysis. One-way ANOVA and Student-Newman-Keuls (SNK) post hoc tests were used to statistically compare differences in rotational stiffness between shoe designs, ankle joint torques at 30 deg rotation, shoe/ankle rotational stiffness, intercept along the rotation axis, and talus motion (external rotation and eversion) relative to the tibia between the paired limbs. Two-way ANOVA and SNK post hoc tests were used to determine the

differences in the torque-rotation data between shoe designs (factor one) at each torque level (factor two) for the shoe stiffness tests, between limbs (factor one) at each rotation level (factor two) for the cadaver tests, and the difference in ligament strains between the flexible and rigid shoes (factor one) in different ligaments (factor two) for the model simulation. In all statistical tests, p values less than 0.05 were considered significant.



Fig. 3 Testing setup. Five-camera Vicon motion capture system (showing only four cameras) and one video camera (not shown) were used to track motions of the talus relative to the tibia.

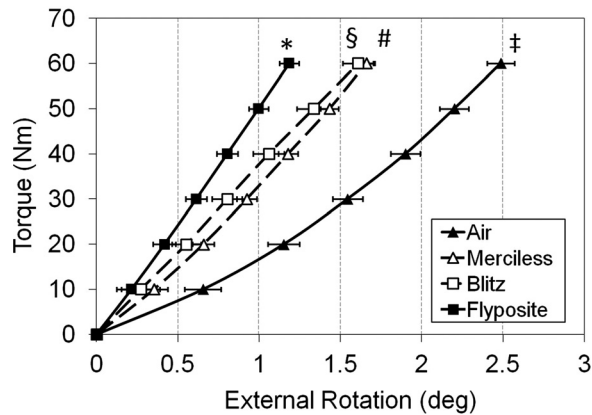


Fig. 4 Torque-rotation curves of the four shoe designs from rotational stiffness tests. Different symbols (‡ # § *) indicate statistically significant differences between shoe designs.

Results

Shoe Stiffness Tests. The pre-torque of 2 Nm was zeroed out by shifting all curves downward in both Fig. 4 for the shoe tests and Fig. 6 for the cadaver tests. Torque-rotation curves demonstrated nearly linear behavior and significant differences between the four shoe designs (Fig. 4). While the Air design showed the lowest rotational stiffness (21.9 ± 2.8 Nm/deg), the Flyposite design had the highest stiffness (50.0 ± 1.7 Nm/deg) (Fig. 5). These two kinds of shoes were then used in the cadaver tests with the Air design being referred as the flexible shoe and the Flyposite design as the rigid shoe. The Merciless and Blitz designs also showed a significant difference in rotational stiffness (34.5 ± 1.9 Nm/deg versus 37.4 ± 2.1 Nm/deg, respectively).

Cadaver Tests. There was an obvious toe region in the torque-rotation curves for both shoe tests (Fig. 6). No significant changes in torque values were observed during the first 5 deg of external rotation. Torque-rotation responses overall were significantly different between limbs, with the limb in the rigid shoe stiffer than that in the flexible shoe (Fig. 6). The shoe/ankle rotational stiffness, defined as the slope of the linear portion of the torque-rotation curves between 10 deg and 30 deg (Fig. 6), was significantly greater for the rigid shoe (1.96 ± 0.24 Nm/deg) than for the flexible shoe (1.65 ± 0.18 Nm/deg) (Table 1). Intercept of linear regression along the rotation axis (Fig. 6) was statistically different

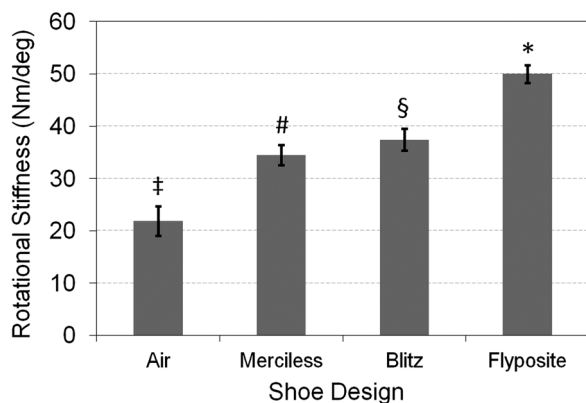


Fig. 5 Rotational stiffness determined from the slopes of torque-rotation curves. Data were averaged across the three cyclic tests and plotted as mean \pm 1 SD. The Air was the least rigid (most flexible) shoe, while the Flyposite was the most rigid design. Different symbols (‡ # § *) indicate statistically significant differences between shoe designs.

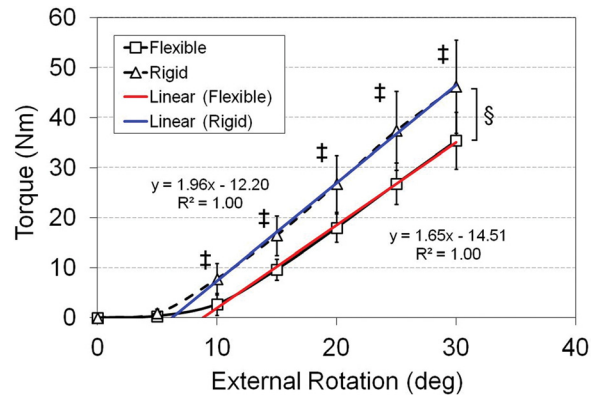


Fig. 6 Torque-rotation curves of cadaveric limbs restrained by the flexible (Air) or the rigid (Flyposite) shoe designs showed a toe region followed by a linear region. Linear regression was performed on the linear portion of the curves between 10° and 30°. The symbol § indicates significant difference between curves. The ‡'s indicate significant differences between limbs at various rotation points.

between the flexible (8.8 ± 1.2 deg) and rigid shoes (6.2 ± 0.9 deg) (Table 1). At 30 deg of external foot rotation, ankle joint torque in the rigid shoe (46.2 ± 9.3 Nm) was statistically higher than that in the flexible shoe (35.4 ± 5.7 Nm) (Table 1).

Motion Analysis. During axial loading of the ankle and prior to external rotation of the foot, talus eversion was noted in both shoes without a significant difference (1.4 ± 0.5 deg for the flexible shoe versus 1.3 ± 0.5 deg for the rigid shoe) (Table 2). In the 30 deg of external foot rotation test, the talus externally rotated more in the rigid shoe (15.9 ± 1.6 deg) than in the flexible shoe (12.1 ± 1.0 deg). Talus eversion, however, was found to be significantly greater in the flexible shoe (5.6 ± 1.5 deg) than in the rigid shoe (1.2 ± 0.8 deg) (Table 2). Medial-lateral translation of the talus was minimal in both shoes (< 1 mm). In addition, external rotation of the talus during axial loading and talus dorsi/plantar flexion were also small and negligible (< 0.5 deg). Temporal profiles showed a statistically different talus rotation in different shoes ($p < 0.001$), with both talus rotations much less than the shoe rotation (Fig. 7).

Model Simulation. While ligament strains in the ADL were at the same level for both shoes ($4.9 \pm 0.4\%$ for the flexible shoe versus $5.2 \pm 0.7\%$ for the rigid shoe), the flexible shoe generated significantly higher strains in the ATiFL ($4.5 \pm 0.4\%$) than the rigid shoe ($2.3 \pm 0.3\%$) (Fig. 8). For both shoes, the ADL experienced higher strains than the ATiFL ($p = 0.043$ for the flexible shoe; $p < 0.001$ for the rigid shoe).

Discussion

This study investigated the rotational stiffness of four football shoe designs. The most flexible and rigid shoes were then used in cadaver experiments in order to investigate the effects of this shoe property on ankle joint torque and talus motion during external rotation of the foot. The talus kinematic data were then input into a generic, computational ankle model for determination of key ankle ligament strains. The results supported the hypotheses that shoes with different rotational stiffness would generate different levels of ankle joint torque and ankle ligament strain patterns. For a given level of external foot rotation, the rigid shoe developed more torque than the flexible shoe. Furthermore, there was a dramatic jump in strain of the ATiFL for the flexible versus the rigid shoe design, while the ADL strain was nearly the same in both shoes. The significant increase in ATiFL strain may be largely due to the greater talus eversion documented for the flexible shoe.

Table 1 Specimen Descriptions and Results from the Cadaver Tests

Specimen	Age	Height (m)	Weight (kg)	Torque at 30 deg rotation (Nm) ^a		Rotational stiffness (Nm/deg) ^b		Intercept along x axis (deg) ^c	
				Flexible	Rigid	Flexible	Rigid	Flexible	Rigid
1	76	1.72	64	39.5 (L)	58.8 (R)	1.75	2.13	9.5	6.6
2	56	1.83	79	36.9 (R)	42.4 (L)	1.48	1.68	8.9	6.4
3	40	1.88	75	34.5 (L)	40.2 (R)	1.71	2.18	7.2	5.3
4	50	1.75	88	37.9 (R)	42.8 (L)	1.84	2.02	10.6	7.7
5	55	1.78	66	24.3 (L)	36.4 (R)	1.39	1.64	7.7	5.2
6	56	1.88	93	39.2 (R)	56.8 (L)	1.74	2.09	8.6	5.9
Mean	56	1.81	77.5	35.4	46.2 ^d	1.65	1.96 ^d	8.8	6.2 ^d
SD	12	0.07	11.6	5.7	9.3	0.18	0.24	1.2	0.9

^aThe left (L) and right (R) limbs were randomly assigned.

^bRotational stiffness was defined as the slope of the linear portion of the torque-rotation curves (between 10° and 30°) in Figure 6.

^cLinear regression of each curve in Figure 6 was intercepted with the rotation (x) axis and the intercept was documented.

^dStatistically different than in the flexible shoe ($p < 0.001$).

Table 2 Talus Motion Relative to the Tibia (mean ± SD) in Different Shoes

Talus motion ^a	Axial loading of 1500 N		Foot at 30° external rotation	
	Flexible	Rigid	Flexible	Rigid
External rotation (deg)	—	—	12.1 ± 1.0	15.9 ± 1.6 ^b
Eversion (deg)	1.4 ± 0.5	1.3 ± 0.5	5.6 ± 1.5	1.2 ± 0.8 ^b

^aNote: Talus external rotation during axial loading (—) and talus dorsi/plantar flexion (not shown) were minimal and negligible (< 0.5°).

^bStatistically different than in the flexible shoe ($p < 0.001$).

These results are supported, in part, by an earlier study from our laboratory showing that during external rotation tests, a shoe with a more pliable upper tended to have its medial edge dig into the turf more than a rigid shoe design [15]. This motion of the more flexible shoe may allow the foot to evert more than a rigid design during external rotation of the foot. In another more recent study by this laboratory, eversion of an axially loaded foot prior to external rotation transferred the site of ligament failure from the ADL to the ATiFL [27]. While all specimens in the current study were initially placed in a neutral position, during external rotation of the foot, there was significantly more coupled eversion of the talus for the flexible shoe design. As might have been expected with a neutral foot, both shoe designs showed the largest strains in the ADL.

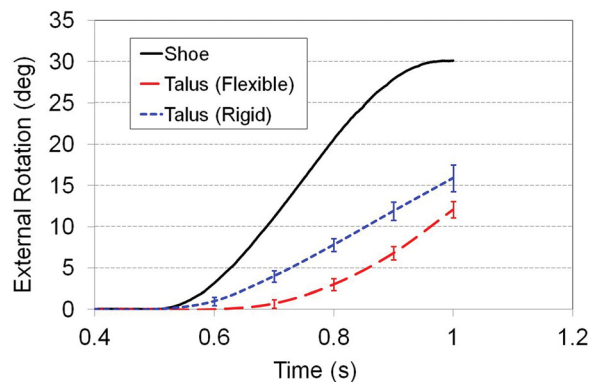


Fig. 7 Comparisons of temporal profiles of external talus rotations in different shoes with the actual shoe rotation (same in all tests) driven by the rotary actuator. All rotations were relative to the tibia.

The mean ankle ligament strains in the ATiFL and ADL from the model analysis of the current study indicated levels of approximately 2.3% and 5.2%, respectively, for the rigid shoe under 30 deg of foot rotation. Interestingly, a previous simulation study in which the cadaver foot was restrained with athletic tape showed a comparable pattern of ligament strains with the ATiFL at 2% and the ADL at 7% under the same conditions of axial load and foot rotation as for the rigid shoe in the current study [22]. A previous study by Verhagen et al. [28], investigating the efficacy for preventive measures on ankle sprains, shows that while the use of tape reduces the incidence of ankle sprains, the efficacy of shoes in preventing the injury is unclear. The data from the current study, however, may suggest some level of parallel restraint to the foot between this method of ankle taping and the more rigid foot-ball shoe design.

In the current study, while the flexible shoe generated less external rotation of the talus relative to the tibia, it resulted in significantly greater talus eversion than using the rigid shoe design. One potential explanation for these contrasting talus motions may be that the more flexible shoe provided less restraint to the subtalar and transverse tarsal joints than the more rigid shoe. This allowed relatively more motion between the talus and the calcaneus, generating foot eversion [21] for the flexible shoe. Furthermore, the flexible shoe also allowed more motion between the forefoot and the hindfoot, producing less axial talus rotation

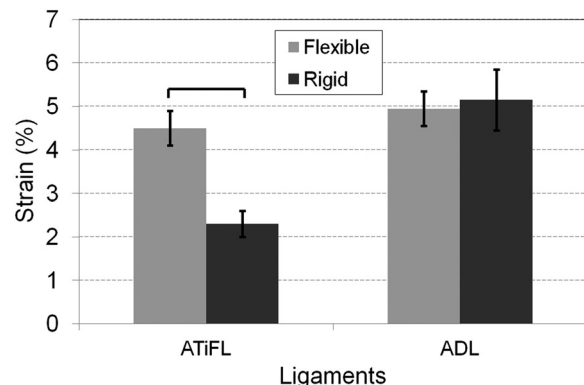


Fig. 8 Ankle ligament strains (mean ± 1 SD) were estimated from a computational model and compared between different shoes at 30° of external foot rotation. Only two ligaments with the highest strains were reported. ATiFL is the anterior tibiofibular ligament, and ADL is the anterior deltoid ligament. The horizontal bar indicates significant difference between shoes. The strain in the ADL was statistically greater than in the ATiFL for both shoe designs.

during external rotation of the foot. In contrast, the more rigid shoe design coupled motion of the foot with the talus during external rotation, but might prevent the coupling of talus eversion with external rotation of the foot that would be expected with an unrestrained foot and ankle condition [29]. Unfortunately, motions of the calcaneus, navicular and cuboid in the shoes were not measured in the current study due to the difficulty in placing marker arrays into those bones. As a result, subtalar and transverse tarsal joint motions were unknown. Cutting holes in the shoes may be a solution in future studies, assuming the consequent alteration in shoe property was minimal.

The current study also suggested a correlation between ankle joint torque and axial talus rotation. For example, at 30 deg of foot/shoe rotation, axial talus rotation in the flexible shoe was 12.1 deg, generating 35.4 Nm of ankle joint torque. In contrast, axial talus rotation in the rigid shoe was 15.9 deg, generating 46.2 Nm of ankle joint torque. Interestingly, the ratio of ankle joint torque to axial talus rotation was similar at 2.9 Nm/deg between shoe designs. This stiffness, which seemed to be independent of shoes, but likely dependent on the given conditions of ankle joint pre-load and rate of external foot rotation, may characterize a structural property of the human ankle. An earlier study by this laboratory shows that the in vivo foot rotational stiffness is 1.1 – 1.5 Nm/deg in terms of axial hindfoot rotation, which might be expected, however, to be greater than talus rotation at the same level of foot rotation [24].

A previous study by Reinschmidt et al. [30] compares tibio-calcaneal motion during running based on skeletal markers with the motion based on external markers attached to the shoe and shank. The study shows that the mean difference between external and skeletal marker-based rotations is 51.2% of the total motion, and therefore concludes that rotations derived from external shoe and shank markers typically overestimate the skeletal tibio-calcaneal kinematics. In contrast, the current study was designed to measure tibio-talar motion during external foot rotation. While no external markers were attached to the shoes in the current study and shoe motion was restrained to internal-external rotation only, shoe rotation was accurately controlled by the testing fixture. Interestingly, the current study also demonstrated a large difference between shoe rotation and talus rotation. For example, at 30 deg of rigid shoe rotation, the average talus rotation was approximately 15.9 deg. In contrast, with the more flexible shoe restraint 30 deg of shoe rotation generated approximately 12.1 deg of talus rotation, showing that shoe design can yield a differing level of restraint to the ankle and may play a role in the potential for ankle joint injury.

While the current studies were limited in that only a few shoe designs were considered and the study was of a subfailure nature, a couple future studies could be envisioned. First, the current study showed that external rotation of the foot/shoe to 30 deg generated ankle ligament strains up to approximately 5%. Future cadaver studies, possibly with a similar experimental setup to vary the levels of foot dorsiflexion and eversion, could rotate the ankle to a failure level to document some effects of football shoe design on the potential for and subsequent location of ankle injury. Secondly, the current experimental setup could be modified to study shoe-surface interface characteristics in order to investigate the potential influence of shoe-surface interface in developing ankle ligament strains as an indication of the potential for location and severity of ankle ligament injury, similar to that previously conducted to study the role of shoe-surface interface on the potential for knee ligament injury [31].

In conclusion, we externally rotated six pairs of cadaver limbs in two different football shoe designs, a flexible shoe and a rigid shoe, and found that while axial talus rotation was significantly greater in the rigid shoe, the flexible shoe generated statistically more talus eversion. The study showed that football shoe design can have an effect on the pattern of ankle ligament strains during external rotation of the foot to potentially influence the location and severity of a subsequent ankle injury. While the current

study was indeed limited in scope, it represents a first step in our attempt to understand the effect of football shoe design on the potential for ankle injury. These studies must also consider the possible implications of football shoe design on player performance and balance this factor with the potential for ankle injury.

Acknowledgment

The authors thank Mr. Clifford Beckett for technical assistance in this study, Mrs. Jean Atkinson for specimen preparation, and Mr. Dean Mueller for the help in procuring the test specimens.

References

- [1] Barker, H. B., Beynon, B. D., and Renstrom, P. A., 1997, "Ankle Injury Risk Factors in Sports," *Sports Med.*, **23**(2), pp. 69–74.
- [2] Hootman, J. M., Dick, R., and Agel, J., 2007, "Epidemiology of Collegiate Injuries for 15 Sports: Summary and Recommendations for Injury Prevention Initiatives," *J. Athl. Train.*, **42**(2), pp. 311–319.
- [3] Wolfe, M. W., Uhl, T. L., Mattacola, C. G., and McCluskey, L. C., 2001, "Management of Ankle Sprains," *Am. Fam. Physician*, **63**(1), pp. 93–104.
- [4] Fong, D. T., Hong, Y., Chan, L. K., Yung, P. S., and Chan, K. M., 2007, "A Systematic Review on Ankle Injury and Ankle Sprain in Sports," *Sports Med.*, **37**(1), pp. 73–94.
- [5] Beynon, B. D., Murphy, D. F., and Alosa, D. M., 2002, "Predictive Factors for Lateral Ankle Sprains: A Literature Review," *J. Athl. Train.*, **37**(4), pp. 376–380.
- [6] Fallat, L., Grimm, D. J., and Saracco, J. A., 1998, "Sprained Ankle Syndrome: Prevalence and Analysis of 639 Acute Injuries," *J. Foot Ankle Surg.*, **37**(4), pp. 280–285.
- [7] Gerber, J. P., Williams, G. N., Scoville, C. R., Arciero, R. A., and Taylor, D. C., 1998, "Persistent Disability Associated with Ankle Sprains: A Prospective Examination of an Athletic Population," *Foot Ankle Int.*, **19**(10), pp. 653–660.
- [8] Guise, E. R., 1976, "Rotational Ligamentous Injuries to the Ankle in Football," *Am. J. Sports Med.*, **4**(1), pp. 1–6.
- [9] Hopkinson, W. J., St Pierre, P., Ryan, J. B., and Wheeler, J. H., 1990, "Syndesmosis Sprains of the Ankle," *Foot Ankle*, **10**(6), pp. 325–330.
- [10] Powell, J. W., and Schootman, M., 1992, "A Multivariate Risk Analysis of Selected Playing Surfaces in the National Football League: 1980 to 1989. An Epidemiologic Study of Knee Injuries," *Am. J. Sports Med.*, **20**(6), pp. 686–694.
- [11] Waterman, B. R., Belmont, P. J. Jr., Cameron, K. L., Svoboda, S. J., Alitz, C. J., and Owens, B. D., 2011, "Risk Factors for Syndesmosis and Medial Ankle Sprain: Role of Sex, Sport, and Level of Competition," *Am. J. Sports Med.*, **39**(5), pp. 992–998.
- [12] Bjerneboe, J. Bahr, R. and Andersen, T. E., 2010, "Risk of Injury on Third-Generation Artificial Turf in Norwegian Professional Football," *Br. J. Sports Med.*, **44**(11), pp. 794–798.
- [13] Dowling, A. V., Corazza, S., Chaudhari, A. M., and Andriacchi, T. P., 2010, "Shoe-Surface Friction Influences Movement Strategies During a Sidestep Cutting Task: Implications for Anterior Cruciate Ligament Injury Risk," *Am. J. Sports Med.*, **38**(3), pp. 478–485.
- [14] Heidt, R. S. Jr., Dornier, S. G., Cawley, P. W., Scranton, P. E. Jr., Losse, G., and Howard, M., 1996, "Differences in Friction and Torsional Resistance in Athletic Shoe-Turf Surface Interfaces," *Am. J. Sports Med.*, **24**(6), pp. 834–842.
- [15] Villwock, M. R., Meyer, E. G., Powell, J. W., Fouty, A. J., and Haut, R. C., 2009, "Football Playing Surface and Shoe Design Affect Rotational Traction," *Am. J. Sports Med.*, **37**(3), pp. 518–525.
- [16] Wannop, J. W., Worobets, J. T., and Stefanyszyn, D. J., 2010, "Footwear Traction and Lower Extremity Joint Loading," *Am. J. Sports Med.*, **38**(6), pp. 1221–1228.
- [17] Nigg, B. M., and Yeadon, M. R., 1987, "Biomechanical Aspects of Playing Surfaces," *J. Sports Sci.*, **5**(2), pp. 117–145.
- [18] Torg, J. S., Quendenfeld, T. C., and Landau, S., 1974, "The Shoe-Surface Interface and its Relationship to Football Knee Injuries," *J. Sports Med.*, **2**(5), pp. 261–269.
- [19] Livesay, G. A., Reda, D. R., and Nauman, E. A., 2006, "Peak Torque and Rotational Stiffness Developed at the Shoe-Surface Interface: The Effect of Shoe Type and Playing Surface," *Am. J. Sports Med.*, **34**(3), pp. 415–422.
- [20] Sarsam, I. M., and Hughes, S. P., 1988, "The Role of the Anterior Tibio-Fibular Ligament in Talar Rotation: An Anatomical Study," *Injury*, **19**(2), pp. 62–64.
- [21] Hertel, J., Denegar, C. R., Monroe, M. M., and Stokes, W. L., 1999, "Talocrural and Subtalar Joint Instability after Lateral Ankle Sprain," *Med. Sci. Sports Exerc.*, **31**(11), pp. 1501–1508.
- [22] Wei, F., Hunley, S. C., Powell, J. W., and Haut, R. C., 2011, "Development and Validation of a Computational Model to Study the Effect of Foot Constraint on Ankle Injury Due to External Rotation," *Ann. Biomed. Eng.*, **39**(2), pp. 756–765.
- [23] Wei, F., Villwock, M. R., Meyer, E. G., Powell, J. W., and Haut, R. C., 2010, "A Biomechanical Investigation of Ankle Injury under Excessive External Foot Rotation in the Human Cadaver," *J. Biomech. Eng.*, **132**(9), 091001.

- [24] Wei, F., Braman, J. E., Weaver, B. T., and Haut, R. C., 2011, "Determination of Dynamic Ankle Ligament Strains from a Computational Model Driven by Motion Analysis Based Kinematic Data," *J. Biomech.*, **44**(15), pp. 2636–2641.
- [25] Grood, E. S., and Suntay, W. J., 1983, "A Joint Coordinate System for the Clinical Description of Three-Dimensional Motions: Application to the Knee," *J. Biomech. Eng.*, **105**(2), pp. 136–144.
- [26] Soutas-Little, R. W., Beavis, G. C., Verstraete, M. C., and Markus, T. L., 1987, "Analysis of Foot Motion During Running Using a Joint Co-Ordinate System," *Med. Sci. Sports Exerc.*, **19**(3), pp. 285–293.
- [27] Wei, F., Post, J. M., Braman, J. E., Meyer, E. G., Powell, J. W., and Haut, R. C., 2012, "Eversion during External Rotation of the Human Cadaver Foot Produces High Ankle Sprains," *J. Orthop. Res.*, pp. (in press).
- [28] Verhagen, E. A., Van Mechelen, W., and De Vente, W., 2000, "The Effect of Preventive Measures on the Incidence of Ankle Sprains," *Clin. J. Sport Med.*, **10**(4), pp. 291–296.
- [29] Funk, J. R., 2011, "Ankle Injury Mechanisms: Lessons Learned from Cadaveric Studies," *Clin. Anat.*, **24**(3), pp. 350–361.
- [30] Reinschmidt, C., Van Den Bogert, A. J., Murphy, N., Lundberg, A., and Nigg, B. M., 1997, "Tibiocalcaneal Motion During Running, Measured with External and Bone Markers," *Clin. Biomech. (Bristol, Avon)*, **12**(1), pp. 8–16.
- [31] Drakos, M. C., Hillstrom, H., Voos, J. E., Miller, A. N., Kraszewski, A. P., Wickiewicz, T. L., Warren, R. F., Allen, A. A., and O'Brien, S. J., 2010, "The Effect of the Shoe-Surface Interface in the Development of Anterior Cruciate Ligament Strain," *J. Biomech. Eng.*, **132**(1), 011003.